Technetium-99m-ECD Brain SPECT in Misery Perfusion

Eku Shimosegawa, Jun Hatazawa, Yasuo Aizawa, Yasuaki Shouji, Takenori Hachiya and Matsutarou Murakami
Department of Radiology and Nuclear Medicine, Research Institute of Brain and Blood Vessels, Akita, Japan

Discordant findings of ^{99m}Tc-methyl cysteinate dimer (^{99m}Tc-ECD) brain distribution have been reported when brain tissue is supplied by excess blood flow. We evaluated changes in ^{99m}Tc-ECD brain activity in the opposing pathological state, in which cerebral blood flow (CBF) is more profoundly impaired than metabolism, and analyzed the relationship of ^{99m}Tc-ECD activity with CBF and metabolism to investigate the dominant regulating factor on ^{99m}Tc-ECD distribution. **Methods:** Twelve patients with unilateral intracranial steno-occlusive diseases were evaluated using dynamic and static ^{99m}Tc-ECD SPECT. Relative ^{99m}Tc-ECD activities and the retention ratio of the affected and unaffected cortices were compared with CBF and oxygen metabolism obtained by PET. Change in the relationships until 1 hr after tracer injection were also analyzed. **Results:** Relative ^{99m}Tc-ECD activity was significantly correlated with CBF, and the highest correlation was obtained for the first minute of imaging ($r = 0.674$, $p < 0.001$). Fifteen minutes after injection, the correlation coefficient with CBF decreased, whereas higher correlation was observed with the parameter of oxygen metabolism ($r = 0.758$–0.815, $p < 0.001$). Changes in the retention ratio were dependent on changes in oxygen metabolism, and the retention ratio for the high oxygen extraction fraction (OEF) area was the same as that for the normal OEF area. **Conclusion:** In addition to CBF, brain distribution on ^{99m}Tc-ECD SPECT images is affected by brain metabolism, especially on delayed images after injection. The degree of discrepancy between CBF and metabolism should be considered when interpreting images of the misery perfusion state.

Key Words: SPECT; steno-occlusive disease; technetium-99m-ECD; PET

J Nucl Med 1997; 38:791–796

Quantitative and semiquantitative cerebral blood flow (CBF) imaging has been used in various clinical situations following the development of more advanced high-resolution SPECT systems and CBF tracers. The clinical utility of ^{99m}Tc-ethyl cysteinate dimer (^{99m}Tc-ECD) has been established in the assessment of cerebral infarction, epilepsy and dementia because of the stable image it provides due to prolonged preservation of brain activity after tracer injection, even in emergency situations or agitated patients, for SPECT studies (*1–5*).

Although ^{99m}Tc-ECD has been validated as a flow tracer after pharmacological and physiological examinations (*6–9*), findings inconsistent with those of quantitative CBF imaging have also been reported in some pathological conditions, especially in the state of uncoupling between brain circulation and metabolism (*1–2,10–11*). In the luxury perfusion state with damaged brain tissue, ^{99m}Tc-ECD activity is decreased when quantitative and qualitative CBF imaging demonstrates normo- or hyperperfusion (*1–2,10–15*). The brain distribution of ^{99m}Tc-ECD in this state, however, would be modified by the alteration of tracer transportation because of the breakdown of the blood-brain barrier. The impairment of the transportation would cause a decrease in ^{99m}Tc-ECD input and/or the leakage of its metabolites, and ^{99m}Tc-ECD activity is suggestive of a complex set of information in addition to changes to the inner retention mechanism of the brain. In view of these difficulties, investigations of the tracer kinetics in the uncoupling state need more explicit models for analysis.

To exclude the effect of the blood-brain barrier breakdown and simplify the retention mechanism of ^{99m}Tc-ECD in the brain, we investigated time-dependent changes in ^{99m}Tc-ECD accumulation in the "misery perfusion" state, in which CBF is more profoundly impaired than metabolism. Misery perfusion is frequently observed in patients with occlusion of the main intracranial artery and indicates a crucial state that may result in irreversible ischemic damage when the perfusion pressure is not sufficient to maintain brain homeostasis (*16*). The brain framework in this state, however, is preserved, including blood vessels, and the retention of ^{99m}Tc-ECD is presumed to directly relate to changes in the inner brain metabolism. In this study, ^{99m}Tc-ECD accumulations on dynamic and static SPECT images were compared to PET images obtained just before the SPECT study.

METHODS

Patients

Twelve patients with unilateral intracranial steno-occlusive disease (8 men, 4 women; age range 26–80 yr; mean age 60.0 ± 17.0 yr) were recruited to participate in this study. A clinical profile of each patient is presented in Table 1. All patients had transient or persistent symptoms of ischemic attack, and the main complaint of the symptoms was hemiparesis in six patients, dysarthria in four patients, numbness in one patient and gait disturbance in one patient. The presence of a unilateral intracranial arterial lesion was confirmed by conventional angiography in ten patients and magnetic resonance angiography (MRA) in two patients; occlusion of the internal carotid artery was documented in four patients, stenosis of the internal carotid artery in one patients, occlusion of the middle cerebral artery in five patients, and stenosis of the middle cerebral artery in two patients. The mean time interval from the initial attack to this study was 45.3 ± 39.7 days.

Midsagittal T1-weighted MRI was first performed before the present PET and SPECT studies to determine the anterior commissure-posterior commissure (AC-PC) baseline. Transaxial T1-weighted and T2-weighted images were obtained 19 planes parallel to the AC-PC line. In no patients did transaxial MRI disclose any morphological damage on the cerebral cortices other than the deep structures of the brain.

Informed consent was obtained from the subjects or their relatives, and the protocol of this study was approved by the PET Research Committee of our institution.

PET Measurement

Regional CBF (rCBF), regional cerebral metabolic rate for oxygen ($rCMRO_2$) and regional oxygen extraction fraction (rOEF)

Received May 21, 1996; revision accepted Sept. 4, 1996.
For correspondence or reprints contact: Eku Shimosegawa, MD, Dept. of Radiology and Nuclear Medicine, Research Institute of Brain and Blood Vessels, 6–10 Senshu-Kubota Machi, Akita 010, Japan.

TABLE 1
Summary of Patient Data

Patient no.	Age (yr)	Sex	Angiographical finding	Main symptom	Interval from initial attack to SPECT-PET study (days)
1	69	M	rt. MCA occlusion	Hemiparesis	48
2	67	M	rt. MCA occlusion	Dysarthria	59
3	72	M	rt. ICA stenosis	Hemiparesis	65
4	59	M	rt. ICA occlusion	Hemiparesis	140
5	47	F	rt. MCA occlusion	Dysarthria	19
6	43	M	rt. MCA stenosis	Hemiparesis	11
7	76	F	lt. MCA stenosis	Dysarthria	101
8	77	F	rt. MCA occlusion*	Hemiparesis	22
9	68	F	lt. MCA occlusion	Numbness	49
10	26	M	rt. ICA occlusion	Hemiparesis	5
11	36	M	rt. ICA occlusion	Dysarthria	12
12	80	M	rt. ICA occlusion*	Gait disturbance	12
Average	60.0 ± 17.0 yr			45.3 ± 39.7 days	

*Angiographical findings were obtained by magnetic resonance angiography.

were measured using a four-ring, seven-slice PET scanner, with in-plane and axial resolutions of 8 and 10 mm, respectively (*17*). To align the PET images to the AC-PC parallel MRI, a lateral cranial radiograph that included the landmark was obtained before the PET study and was adjusted to the AC-PC line by measuring the angle produced by the orbitomeatal (OM) line. After positioning of the head for the PET measurement, another landmark was located on the patient's cheek parallel to the laser beam line to match the PET planes to the SPECT planes.

Before emission scanning, a transmission scan using a ^{68}Ga-^{68}Ge line source was performed to correct tissue attenuation. The rCBF was calculated by autoradiographic method with 90-sec scanning after intravenous administration of 1110 MBq of ^{15}O-water. Continuous arterial blood sampling and beta-ray monitoring with a scintillator were conducted throughout PET scanning using a catheter implanted into the radial artery to obtain the arterial input function. Measurements of $rCMRO_2$ and rOEF were performed with 1-min inhalation of 6105 MBq/min of ^{15}O-labeled molecular oxygen ($^{15}O_2$ gas) and 1-min inhalation of 5180 MBq/min of ^{15}O-labeled carbon monoxide ($C^{15}O$ gas). The arterial input function of $^{15}O_2$ gas was obtained by continously withdrawing blood throughout scanning. Arterial blood sampling for the input function of $C^{15}O$ gas was performed three times during the study. Quantification for $rCMRO_2$ and rOEF was performed after blood volume correction according to the $C^{15}O$ gas inhalation data. Other details regarding the PET procedure have been described elsewhere (*18*).

Dynamic and Static SPECT

After decay of ^{15}O radioactivity in the brain to background levels, dynamic and static SPECT studies were performed on the day of the PET measurement. The continous cylindrical ring scanner provides scans in 16 dynamic and 31 static tomographic transaxial planes. The in-plane and axial spatial resolution obtained using the all-purpose (A-P) and the high-resolution (H-R) collimator was 13 and 12 mm, respectively, and 26 and 21 mm, respectively. Before the SPECT study, line marks were placed on the patient's cheek before the PET study and the patient's head was adjusted to the transaxial and midsagittal light beams of the SPECT system according to these landmarks. Dynamic scanning started immediately after 30 sec manual administration of ^{99m}Tc-ECD

TABLE 2
Averaged rCBF, $rCMRO_2$ and rOEF of Affected and Unaffected Cortices

	rCBF (ml/100 ml/min)		$rCMRO_2$ (ml/100 ml/min)		rOEF	
Patient no.	Affected cortex	Unaffected cortex	Affected cortex	Unaffected cortex	Affected cortex	Unaffected cortex
1	22.1	30.2	1.77	2.32	0.57	0.55
2	23.3	28.0	2.74	3.39	0.47	0.44
3	38.1	41.9	2.64	2.73	0.39	0.37
4	38.6	32.3	2.29	3.09	0.31	0.37
5	31.7	43.8	2.72	3.35	0.65	0.57
6	37.9	41.1	2.91	2.97	0.42	0.39
7	34.2	44.3	2.92	3.12	0.59	0.59
8	34.5	41.3	2.64	2.71	0.60	0.61
9	18.0	34.6	2.14	2.71	0.83	0.57
10	40.4	53.6	3.67	3.85	0.56	0.45
11	28.7	49.1	2.67	3.16	0.62	0.42
12	20.2	26.3	1.93	2.23	0.59	0.52
Average	30.6 ± 7.9*	38.9 ± 8.6*	2.59 ± 0.51†	2.97 ± 0.46†	0.55 ± 0.14‡	0.47 ± 0.07‡

*$p < 0.002$.
†$p < 0.001$.
‡$p < 0.01$.

(1110 MBq) into the antecubital vein. Using the A-P collimator, sequential 1-min/1-frame dynamic scanning was performed for 10 min, and a total of 10 frames was obtained. Static data were collected for 10 min using the H-R collimator, and 3–5 series of static scans were acquired until 1 hr after tracer injection; the mid time for each was 15 min (n = 22), 25 min (n = 20), 35 min (n = 22), 45 min (n = 24) and 55 min (n = 18). The raw dynamic and static SPECT data were transferred to an MV-7890 SH processing system and were respectively reconstructed on a 64 × 64 and a 128 × 128 image matrix using Butterworth filtered backprojection. Data for a pool phantom containing 110–220 MBq ^{99m}Tc were applied to the attenuation correction of dynamic SPECT, and radial postcorrection method was used for that of static SPECT (*19*). Scatter radiation was not corrected because the appropriate method was not included in the system. Linearization of ^{99m}Tc-ECD activity for the correction of hyperperfused area was not performed because of the lack of an established correction method (*20*). For the coordination of some methodological differences between dynamic and static SPECT scan, i.e., the types of collimators used, matrix size and attenuation correction method for image reconstruction, an uniform cylindrical phantom (16 cm in diameter) containing 111 MBq of ^{99m}Tc was scanned according to the same protocol, and the correction factor was multiplied by the value for decay-corrected static SPECT radioactivity.

ROI Selection and Data Analyses

On both the PET and SPECT images, the same regions of interests (ROIs) were located on the affected cortices in the territory of the middle cerebral artery, where no morphological change was identified on the reference MR image. Each ROI was oval-shaped and 3 × 5 cm in size. The mirror ROI was applied to the contralateral unaffected cortices. Other oval ROIs 2 × 3 cm in size were placed on the cerebellar cortex of the ipsilateral affected side to normalize cortical activities on the PET and SPECT images.

We first analyzed sequential changes in the relationship between ^{99m}Tc-ECD activity and PET values. Averaged ^{99m}Tc-ECD activity, rCBF and $rCMRO_2$ of affected and unaffected cortices were each divided by the corresponding cerebellar values for the reference and were defined as the relative ^{99m}Tc-ECD activity and PET values. Correlation coefficients were calculated for the relation of relative ^{99m}Tc-ECD activity for each scan time (1, 7, 15, 25, 35, 45, 55 min) to relative rCBF or $rCMRO_2$, respectively.

The time course change in the relationship between the retention ratio of ^{99m}Tc-ECD and the PET values was then evaluated. The retention ratio of ^{99m}Tc-ECD is expressed as:

$$\text{retention ratio} = \frac{\text{averaged } ^{99m}\text{Tc—ECD activity of the affected or unaffected cortex}}{\text{averaged cerebellar activity of the affected side within first 5 min}}.$$

The retention ratio of ^{99m}Tc-ECD at each of the early and delayed scanning times (7 min, 15 min and 45 min) was plotted against rCBF, $rCMRO_2$ or rOEF, and the linearity and correlation of each relationship was evaluated. A p value <0.05 was considered significant.

RESULTS

The PET measurements demonstrated a significant decrease in the blood supply and metabolism between the affected and unaffected cortices. Table 2 shows the PET results for each patient and the averaged rCBF, $rCMRO_2$ and rOEF of the affected and unaffected cortices of all patients. The difference in averaged rCBF, $rCMRO_2$ and rOEF between the affected and unaffected cortices was statistically significant, based on paired Student's t-test ($p < 0.002$, $p < 0.001$ and $p < 0.01$, respectively).

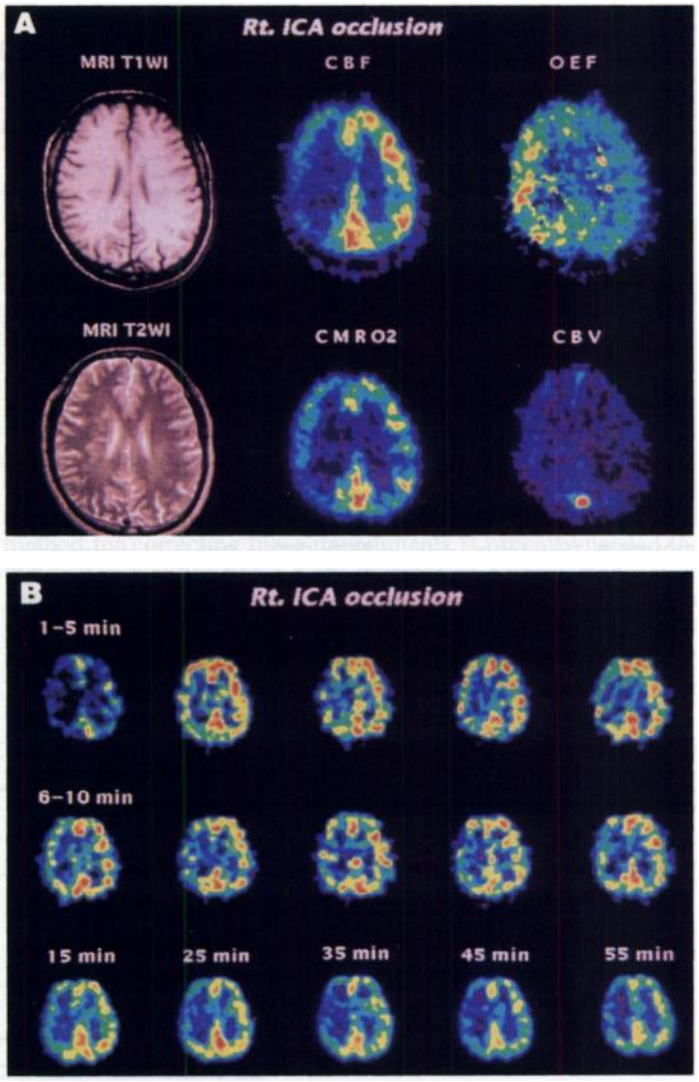

FIGURE 1. (A) MRI and PET images in Patient 11. T2-weighted MRI obtained 12 days after initial symptom onset (left column) demonstrates an infarction observed only in the right deep white matter and that the peri-infarct cortices remain morphologically intact. High OEF of the affected cortex indicates uncoupling between CBF and oxygen metabolism (right column). (B) Dynamic and static ^{99m}Tc-ECD SPECT images in the corresponding plane in the same patient show slightly diminished contrast between the affected and unaffected cortices 2 min after injection compared to the initial dynamic SPECT and PET CBF image.

The MR, PET and ^{99m}Tc-ECD SPECT images of a representative patient (Patient 11) with an occluded right internal cerebral artery show that the dynamic ^{99m}Tc-ECD SPECT image at 1 min provides the closest contrast to PET CBF (Fig. 1). Two minutes after tracer injection, the contrasts in ^{99m}Tc-ECD activity were stable and slightly diminished compared to those on the initial dynamic SPECT and PET CBF images.

Figure 2 shows time-activity curves of ^{99m}Tc-ECD of the affected and unaffected cortices in the same patient. The brain activity of ^{99m}Tc-ECD plateaued within 2 min after tracer injection. The difference between the affected and unaffected cortices was maximum on the first 1-min image. Thereafter a constant difference in activity was maintained until 1 hr.

The correlation coefficients of the relationship between the averaged relative ^{99m}Tc-ECD activity and relative rCBF or $rCMRO_2$ of the affected and unaffected cortices give a specific pattern of time-dependent change (Fig. 3 and Table 3). The strongest linearity between relative ^{99m}Tc-ECD and relative rCBF was observed at 1 min postinjection ($r = 0.674$, $n = 24$, $p < 0.001$). After 15 min, the coefficient for the relation with

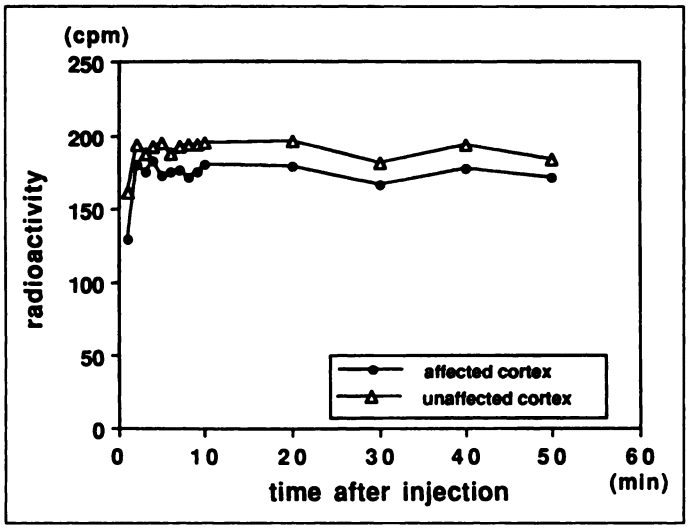

FIGURE 2. Time-activity curve of ^{99m}Tc-ECD in Patient 11 demonstrates brain tracer input plateaus within 2 min after tracer injection and shows stable activity until 1 hr. The maximum difference of the activity between the affected and unaffected cortices is seen during the first minute of imaging.

the relative rCBF decreased to below 0.6 ($r = 0.493–0.574$, $n = 18–24$, $p < 0.05–0.01$), whereas stronger correlations were observed with relative $rCMRO_2$ ($r = 0.758–0.815$, $n = 18–24$, $p < 0.001$). The difference between the correlation coefficient of ECD versus rCBF to that of ECD versus $rCMRO_2$, however, was not statistically significant at any SPECT scan time because of the small study population.

The retention ratio of ^{99m}Tc-ECD gradually decreased after tracer injection. The averaged retention ratio of the affected and unaffected cortices was 0.845 ± 0.055 at 7 min, 0.826 ± 0.059 at 15 min, 0.843 ± 0.053 at 25 min, 0.811 ± 0.058 at 35 min, 0.801 ± 0.062 at 45 min and 0.800 ± 0.056 at 55 min postinjection, respectively. Figure 4 illustrates the relationships between the retention ratio of ^{99m}Tc-ECD and PET parameters at 7 and 45 min after injection. The averaged retention ratio increased linearly, with more significant changes in $rCMRO_2$ than rCBF. The highest correlation was observed with $rCMRO_2$ at 45 min ($y = 0.52+1.12x$, $r = 0.651$, $p < 0.001$, $n = 24$). The retention ratio was constant against the change of rOEF and thus did not show a correlation with rOEF (Fig. 4C and 4F). The cortex with high rOEF, therefore, showed the same retention ratio compared to that with normal rOEF despite decreased CBF.

DISCUSSION

Brain accumulation of a flow tracer is influenced by various regulating factors, which are dependent on the scan time after tracer injection. In the early phase of tracer injection, the first-pass extraction fraction would greatly contribute to the brain tracer distribution. When the fraction of the tracer extracted from the blood into the brain is high and rapid scanning is sufficiently feasible to obtain the initial slope of the brain tracer input , the image would be closer to CBF than at later times after tracer injection. Although the extraction of ^{99m}Tc-ECD in experimental studies is 77%, which is relatively low compared to that of other SPECT imaging agents (*8*), scanning in the very early phase after injection is less influenced by complicated interactions of other factors, i.e., backdiffusion of tracer from the lipophilic component in the brain to the blood or metabolic products in the blood. Backdiffusion of ^{99m}Tc-ECD is less pronounced compared to ^{99m}Tc-HMPAO (*21*). The arterial input 5 min after injection is negligible, because the metabolic products of ^{99m}Tc-ECD do not cross the blood-brain barrier (*8,9*). The good correlation between the

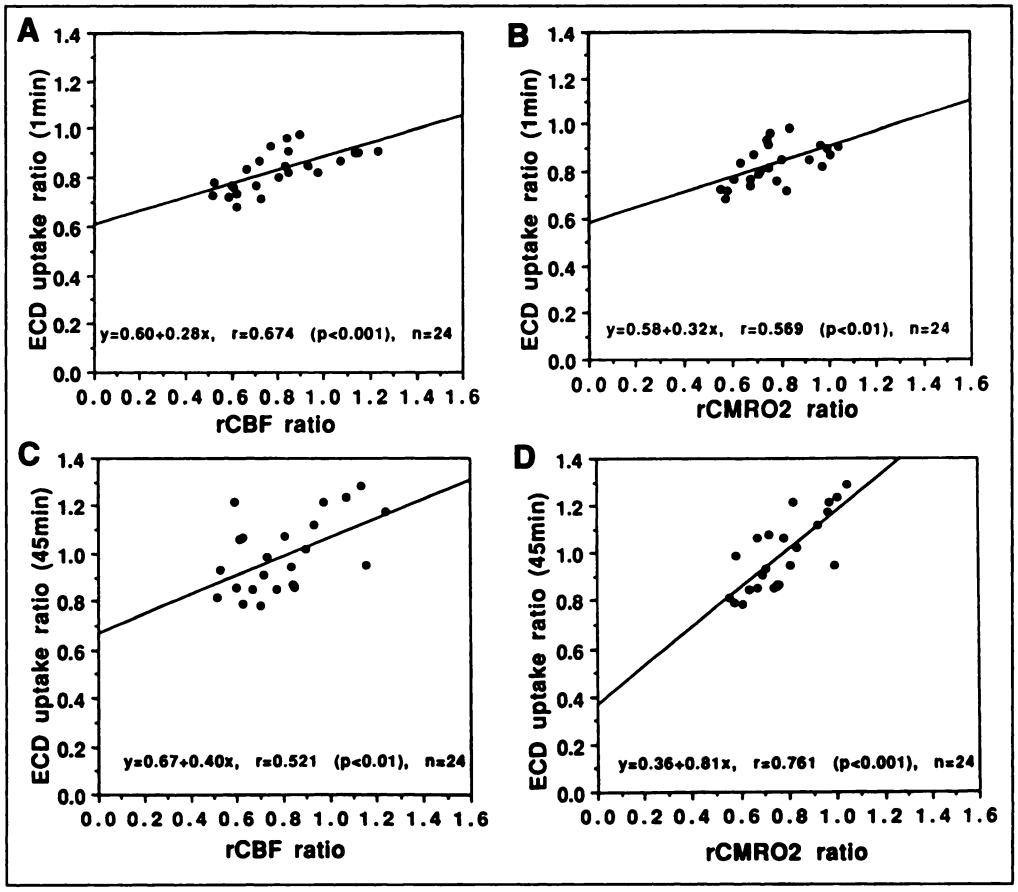

FIGURE 3. The relationship between averaged relative ^{99m}Tc-ECD activity at 1 min or 45 min and the relative rCBF (A,C) or $rCMRO_2$ (B,D). The strongest linearity between relative ^{99m}Tc-ECD activity and rCBF is noted in the early phase after tracer injection, whereas correlation in the delayed phase is higher with $rCMRO_2$ than rCBF.

TABLE 3
Relationship Between Relative Technetium-99m-ECD Activity and Relative PET Values

SPECT scan time (min)	No.	rCBF		$rCMRO_2$	
		r	Significance	r	Significance
1	24	0.674	$p < 0.001$	0.569	$p < 0.01$
7		0.561	$p < 0.01$	0.559	$p < 0.01$
15	22	0.493	$p < 0.05$	0.758	$p < 0.001$
25	20	0.574	$p < 0.01$	0.815	$p < 0.001$
35	22	0.567	$p < 0.01$	0.814	$p < 0.001$
45	24	0.521	$p < 0.01$	0.761	$p < 0.001$
55	18	0.531	$p < 0.05$	0.789	$p < 0.001$

r = correlation coefficient.

relative activity of ^{99m}Tc-ECD and relative CBF within 5 min after injection observed in this study indicates the validity of ^{99m}Tc-ECD SPECT in representing CBF in this phase. It may also may provide an image more closely corresponding to CBF when low extraction is corrected appropriately. Other confounding factors, i.e., scatter radiation and tissue attenuation, reduce the reliability of correlation and linearity and would have an important adverse effect on quantitative CBF images. A method for correcting these impediments is urgently needed to that better quality SPECT CBF images can be produced.

Five minutes after injection, a change in retention likely has a dominant effect on brain ^{99m}Tc-ECD activity. Although the statistical significance of the correlation coefficients between ^{99m}Tc-ECD activity and the PET parameters could not be

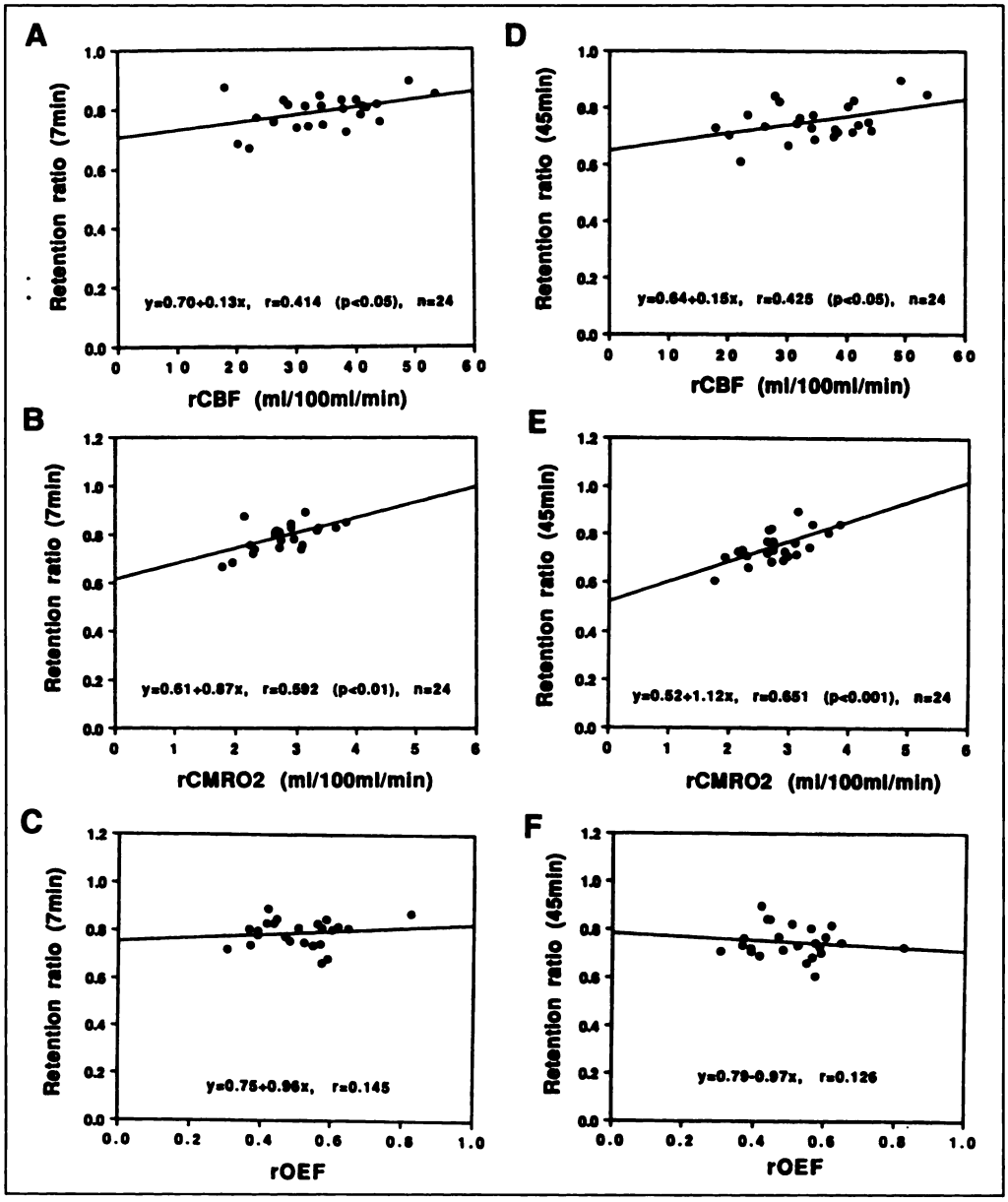

FIGURE 4. Relationship between the retention ratio at 7 min or 45 min and rCBF (A,D), $rCMRO_2$ (B,E) or OEF (C,F). An area with high rOEF value (above 0.6) shows the same retention ratio compared to that with normal rOEF value.

achieved in this study, relative ^{99m}Tc-ECD activities in the brain 15 min after injection demonstrated higher correlation with changes in oxygen metabolism than those of CBF. Furthermore, the retention ratio of ^{99m}Tc-ECD diminished according to decreases in oxygen metabolism. However, it was relatively stable with changes in CBF. The retention ratio in the high OEF cortex was the same as that in the normal OEF cortex, which indicates that retention of ^{99m}Tc-ECD in the area with misery perfusion is the same mechanism as that in coupled perfusion. The contrast on the delayed ^{99m}Tc-ECD SPECT image would be mainly determined not by changes in CBF but by internal metabolic alteration. Delayed images may provide a mix of information that reflects metabolism and CBF. Further study in a larger population may provide more definite confirmation of our findings.

Shishido et al. (*2*) reported that the washout ratio of ^{99m}Tc-ECD versus changes in rCBF or $rCMRO_2$ was 0.8 and stable in nine patients with cerebrovascular disease. In their study, they used the averaged activity from 5–32 min of imaging for normalization in estimating washout, and the ratio would have already been affected by the metabolic factor in this phase. The retention of ^{99m}Tc-ECD activity in the brain is assumed to be regulated by enzymatic activity involved in ester hydrolysis, which reaction seems to be diffusely distributed in the primate brain (*8*). Ester hydrolysis by enzymes and conversion from a lipophilic compound to a hydrophilic monoester-monoacid or diacid compound are suggested as the main retention mechanism of ^{99m}Tc-ECD (*9*), and 65%–74% of these polar metabolites in the primate brain are thought to be found in the cytosol (*8,22*). Since the blood-brain barrier was intact in this study and the transport system of ^{99m}Tc-ECD itself was probably not altered in the morphologically preserved brain tissue, the decreased retention is less related to leakage of hydrophilic compounds from the cytosol to the extracellular space. Furthermore, the averaged $rCMRO_2$ of the affected cortex is 2.59 ± 0.51 ml/100 ml/min, which was slightly lower than the previously published control value (*18*), suggesting a less marked inconsistency between enzymatic activity of ^{99m}Tc-ECD in the cytosol and intracellular oxygen metabolism. Although no direct relationship between ester hydrolysis and intracellular oxygen metabolism has been elucidated, the present result revealed that a change in brain metabolism has a greater influence on the distribution of ^{99m}Tc-ECD than that of CBF on delayed SPECT images. Therefore, scanning time should be considered in pathological states in which the blood supply is impaired despite metabolic preservation.

CONCLUSION

Although a correlation between ^{99m}Tc-ECD activity and CBF is observed throughout dynamic and static scanning, brain distribution of ^{99m}Tc-ECD in SPECT is more strongly related to oxygen metabolism than to CBF 15 min after tracer injection. The ^{99m}Tc-ECD brain SPECT image during misery perfusion, as well as that during luxury perfusion, conveys a complex set of information that is dependent on scan time. Additional verification by hyper-dynamic scanning in the early phase or assessment of vasoreactivity may be necessary for image interpretation when there are discrepancies between blood supply and brain metabolism.

ACKNOWLEDGMENTS

We thank the members of the department of radiology and nuclear medicine for technical advice and support. We also thank Daiichi Radioisotope Laboratories, Ltd., Tokyo, Japan, for providing the ^{99m}Tc-ECD used in this study.

REFERENCES

1. Lassen NA, Sperling B. Technetium-99m-bicisate reliably images CBF in chronic brain diseases but fails to show reflow hyperemia in subacute stroke: report of a multicenter trial of 105 cases comparing ^{133}Xe and ^{99m}Tc-bicisate (ECD, Neurolite) measured by SPECT on the same day. *J Cereb Blood Flow Metab* 1994;14(suppl 1):S44–S48.
2. Shishido F, Uemura K, Murakami M, et al. Cerebral uptake of ^{99m}Tc-bicisate in patients with cerebrovascular disease in comparison with CBF and $CMRO_2$ measured by positron emission tomography. *J Cereb Blood Flow Metab* 1994;14(suppl 1):S66–S75.
3. Walderman G, Walovitch RC, Andersen AR, et al. Technetium-99m-bicisate (Neurolite) SPECT brain imaging and cognitive impairment in dementia of the Alzheimer type: a blinded read of image sets from a multicenter SPECT trial. *J Cereb Blood Flow Metab* 1994;14(suppl 1):S99–S105.
4. Menzel C, Grünwald F, Hufnagel A, et al. Temporal and frontal lobe epilepsy: evaluation of Tc-99m-ECD for ictal and interictal rCBF brain SPECT [Abstract]. *J Nucl Med* 1995;36(suppl):72P.
5. Menzel C, Grünwald F, Steidele S, et al. Childhood epilepsy; detection of frotal and temporal foci using Tc-99m-ECD [Abstract]. *J Nucl Med* 1995;36(suppl):84P.
6. Vallabhajosula S, Zimmerman RE, Picard M, et al. Technetium-99m-ECD: a new brain imagning agent: in vivo kinetics and biodistribution studies in normal human subjects. *J Nucl Med* 1989;30:599–604.
7. Holman BL, Hellman RS, Goldsmith SJ, et al. Biodistribution, dosimetry and clinical evaluation of technetium-99m ethyl cysteinate dimer in normal subjects and in patients with chronic cerebral infarction. *J Nucl Med* 1989;30:1024–1989.
8. Walovitch RC, Hill TC, Garrity ST, et al. Characterization of technetium-99m-L, L-ECD for brain perfusion imaging, Part 1: pharmacology of technetium-99m-ECD in nonhuman primates. *J Nucl Med* 1989;30:1892–1901.
9. Walovitch RC, Franceschi M, Picard M, et al. Metabolism of ^{99m}Tc-L, L-ethyl cysteinate dimer in healthy volunteers. *Neuropharmacology* 1991;30:283–292.
10. Tsuchida T, Nishizawa S, Yonekura Y, et al. SPECT images of technetium-99m-ethyl cysteinate dimer in cerebrovascular diseases: comparison with other cerebral perfusion tracers and PET. *J Nucl Med* 1994;35:27–31.
11. Shishido F, Uemura K, Inugami A, et al. Discrepant ^{99m}Tc-ECD images of CBF in patients with subacute cerebral infarction: a comparison of CBF, $CMRO_2$ and ^{99m}Tc-HMPAO imaging. *Ann Nucl Med* 1995;9:161–166.
12. Nakagawara J, Nakamura J, Takeda R, et al. Assessment of postischemic reperfusion and diamox activation test in stroke using ^{99m}Tc-ECD SPECT. *J Cereb Blood Flow Metab* 1994;14(suppl 1):S49–S57.
13. Tamagac F, Moretti JL, Defer G, Weinmann P, Roussi A, Cesaro P. Nonmatched images with ^{123}I-IMP and ^{99m}Tc-bicisate single-photon emission tomgraphy in the demonstration of focal hyperaemia during the subacute phase of an ischaemic stroke. *Eur J Nucl Med* 1994;21:254–257.
14. Moretti JLM, Tamagac F, Weinmann P, et al. Early and delayed brain SPECT with technetium-99m-ECD and iodine-123-IMP in subacute strokes. *J Nucl Med* 1994;35: 1444–1449.
15. Sato J, Shuke N, Ishikawa Y, et al. Discordant brain distribution between Tc-99m-ECD and Tc-99m-HMPAO: assessment with Tc-99m-ECD dynamic SPECT [Abstract]. *J Nucl Med* 1995;36:244P.
16. Baron JC, Bousser MG, Rey A, Guillard A, Comar D, Castaigne P. Reversal of focal "misery-perfusion syndrome" by extra-intracranial arterial bypass in hemodynamic cerebral ischemia: a case study with ^{15}O positron emission tomography. *Stroke* 1981;12:454–459.
17. Iida H, Miura S, Kanno I, et al. Design and evaluation of Headtome IV: a whole-body positron emission tomograph. *IEEE Trans Nucl Sci* 1989;36:1006–1010.
18. Hatazawa J, Fujita H, Kanno I, et al. Regional cerebral blood flow, blood volume, oxygen extraction fraction and oxygen utilization rate in normal volunteers measured by the autoradiographic technique and the single breath inhalation method. *Ann Nucl Med* 1995;9:15–21.
19. Tanaka E, Toyama H, Murayama H. Convolutional image reconstruction for quantitative single photon emission computed tomography. *Phys Med Biol* 1984;29:1489–1500.
20. Lassen NA, Andersen AR, Freiberg L, Paulson OB. The retention of ^{99m}Tc/DL-HMPAO in human brain after intracarotid bolus injection: a kinetic analysis. *J Cereb Blood Flow Metab* 1988;8:S13–S22.
21. Friberg L, Andersen AR, Lassen NA, Holn S, Dam M. Retention of ^{99m}Tc-bicisate in the human brain after intracarotid injection. *J Cereb Blood Flow Metab* 1994;14(suppl 1):S19–S27.
22. Walovitch RC, Cheesman EH, Maheu LJ, Hall KM. Studies of the retention mechanism of the brain perfusion imaging agent ^{99m}Tc-bicisate (^{99m}Tc-ECD). *J Cereb Blood Flow Metab* 1994;14(suppl 1):S4–S11.